

SSC MAGNET CRYOSTAT SUSPENSION SYSTEM DESIGN

T.H. Nicol, R.C. Niemann and J.D. Goncsy

Fermi National Accelerator Laboratory
Batavia, Illinois

ABSTRACT

The design of the cryostat for the Superconducting Super Collider (SSC) dipole magnets has largely been driven by the design of the cold mass suspension and anchor systems. Rigorous structural requirements in combination with low allowable heat loads have resulted in a suspension system that represents a significant departure from current superconducting magnet design practice both in performance concept and materials selection. This paper presents a summary of the suspension and anchor system designs being employed in the SSC.

INTRODUCTION

The suspension system in a superconducting magnet performs two essential functions. First, it resists internally and externally generated structural loads imposed on the cold mass assembly ensuring that the position of that assembly is stable over the operating life of the magnet. Second, it serves to insulate the cold mass from heat conducted from the outside world.

To satisfy the first function the normal operating stresses in the suspension system must be low enough to avoid creep in the component materials yet sufficient reserve strength must exist to handle loads imposed during shipping and handling of the magnet assembly, seismic excitations, and internally generated quench loads. To satisfy the second function in some optimal way we must size the suspension components to just meet the structural requirements and utilize materials that offer a good compromise between mechanical strength and thermal impedance. Table 1¹ summarizes the structural and thermal loads considered during the design of the suspension system for the SSC.

Table 1. SSC Dipole Structural and Thermal Load Summary

Shipping and handling loads:	vertical	2.0 G
	lateral	1.0 G
	axial	1.5 G
Seismic load guidelines:	Nuclear Regulatory Guide 1.61 vertical and horizontal spectra scaled by 0.3	
Maximum axial quench load:		11360 kg
Budgeted conduction heat loads per magnet:	80 K	7.20 W
	20 K	0.82 W
	4.5 K	0.12 W

DESIGN DEVELOPMENT

Support Post

Several candidate support systems were considered during the early development stages of the SSC.³ A reentrant post assembly was ultimately selected for its superior mechanical and thermal performance. Fig. 1 is a cross section through a typical SSC support post. Its design has been previously described in some detail.^{3,5} Briefly, it consists of two concentric composite tubes; one operating between 300 K and 80 K, the other between 80 K and 4.5 K. The connection between these inner and outer tubes is via a metallic tube located in the annular space between them. It connects the top of the outer tube to the bottom of the inner tube and allows the inner tube to reenter the outer, increasing the total conductive heat path and accounting for its 'folded' construction. All of the metal to composite joints are effected by sandwiching the composite tubes between metallic discs and rings. Clamping forces are generated by shrink fits at all joints.^{3,5} No other mechanical or chemical bonds are made.

Of interest here is some detail regarding the size and material selection for the inner and outer composite tubes. Given the notation in Fig. 2, consider three components of stress acting at points 1 and 2; the points of maximum bending stress in tubes 1 and 2, respectively. The three stresses are induced by: 'g' forces acting at the cold mass centerline, denoted by F_g , quench forces acting at the top of the post, denoted by F_q , and the weight of the cold mass, denoted by W . Given this notation, the total stress acting at point 1 is given by

$$\sigma_1 = \frac{M_{g1}d_1}{2I_1} + \frac{M_{q1}d_1}{2I_1} - \frac{W}{A_1} \quad (1)$$

where M_{g1} = bending moment at point 1 due to F_g
 M_{q1} = bending moment at point 1 due to F_q
 W = weight of the cold mass assembly (per support)
 d_1 = diameter of tube 1
 I_1 = section modulus of tube 1
 A_1 = cross sectional area of tube 1

Similarly for point 2,

$$\sigma_2 = \frac{M_{g2}d_2}{2I_2} + \frac{M_{q2}d_2}{2I_2} - \frac{W}{A_2} \quad (2)$$

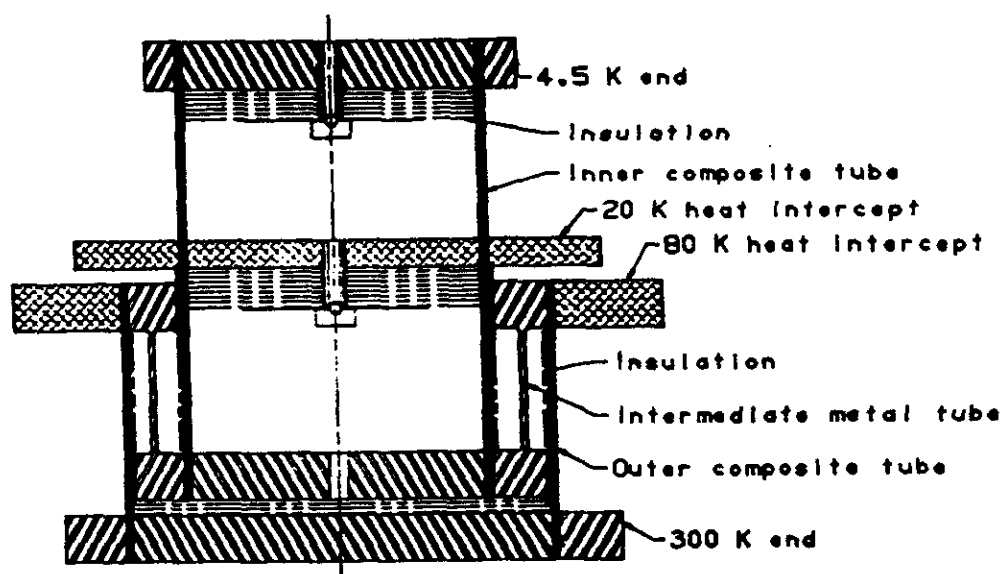


Fig. 1. Cross section through an SSC support post.

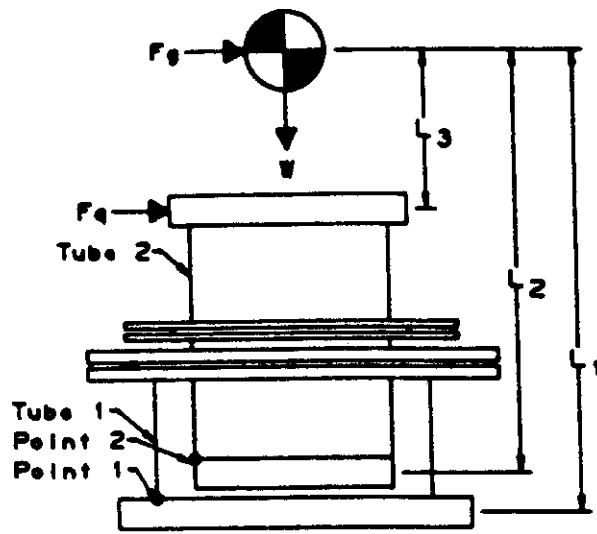


Fig. 2. SSC support post design analysis notation.

Bending moments M_{s1} , M_{q1} , M_{s2} , and M_{q2} are related to F_g , F_q , L_1 , L_2 , and L_3 by

$$\begin{aligned} M_{s1} &= F_g(L_1) \\ M_{q1} &= F_q(L_1-L_3) \\ M_{s2} &= F_g(L_2) \\ M_{q2} &= F_q(L_2-L_3) \end{aligned}$$

So (1) and (2) may be rewritten as

$$\sigma_1 = \frac{F_g L_1 d_1}{2I_1} + \frac{F_q (L_1 - L_3) d_1}{2I_1} - \frac{W}{A_1} \quad (3)$$

and

$$\sigma_2 = \frac{F_g L_2 d_2}{2I_2} + \frac{F_q (L_2 - L_3) d_2}{2I_2} - \frac{W}{A_2} \quad (4)$$

To produce an optimum design using (3) and (4), σ_1 and σ_2 must be equated to the ultimate strength for the materials used of tubes 1 and 2. However, a thin walled tube may fail due to elastic instability (local buckling) at a stress below the ultimate. Elastic instability in thin wall tubes is determined by⁴

$$\sigma_{ei} = \frac{2Et}{\sqrt{3} \sqrt{1-\nu^2} d}$$

where σ_{ei} = stress at which elastic instability occurs
 E^i = elastic modulus
 t = wall thickness
 ν = Poisson's ratio
 d = tube diameter

Our own tests show that the above expression must be derated by approximately 1.5 to agree with results on actual tube material. For tubes 1 and 2 this yields

$$\sigma_{ei1} = \frac{2E_1 t_1}{1.5 \sqrt{3} \sqrt{1-\nu_1^2} d_1} \quad (5)$$

and

$$\sigma_{ei2} = \frac{2E_2 t_2}{1.5 \sqrt{3} \sqrt{1-\nu_2^2} d_2} \quad (6)$$

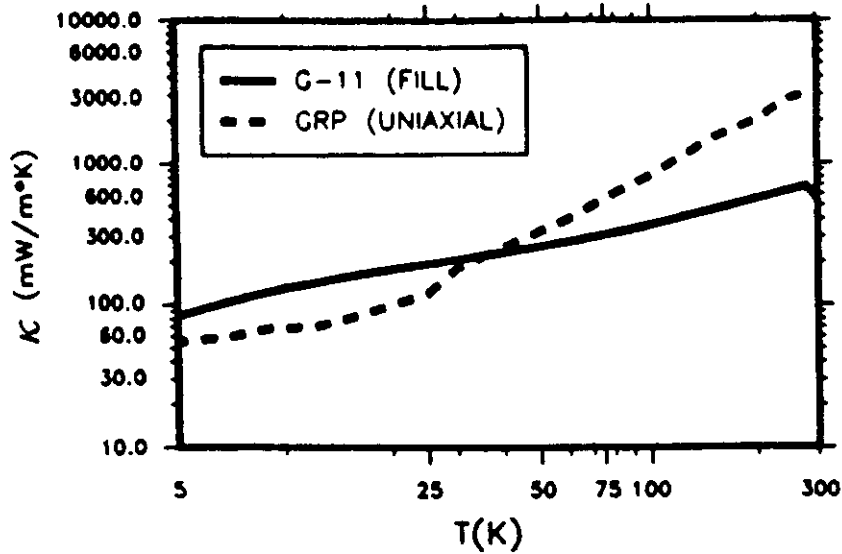


Fig. 3. Thermal conductivity of G-11CR and GRP tube material.

The complete optimization process entails use of (3), (4), (5), and (6). In principle we could optimize with respect to any aspect of the post geometry. In our case the tube lengths are determined more by other cryostat components than by optimization criteria and in the current configuration the structural and thermal performance parameters are not very sensitive to small changes in the tube diameters. Our final optimization is with respect to the thicknesses of tubes 1 and 2, t_1 and t_2 , respectively. Note that although they do not appear explicitly in (3) and (4), t_1 and t_2 are implicit in the expressions for I and A.

Given the properties for candidate materials, a general post geometry, and specified load constraints, we solve equations (3) and (4) for t_1 and t_2 , respectively. Next, we replace the left sides of (3) and (4) with (5) and (6), respectively; again solving for t_1 and t_2 .

The materials selected by this process were NEMA G-11CR for tube 1 and graphite reinforced plastic (GRP) for tube 2. GRP exhibits structural performance superior to that of G-11CR, but has significantly higher thermal conductivity between 300 K and 40 K (see Fig. 3^{4,6}). This makes it undesirable for use in tube 1 which operates between 300 K and 80 K, but potentially attractive for tube 2 operating between 80 K and 4.5 K.

The SSC cryostat contains five support posts; five being the number that limits sag in the cold mass assembly to less than 0.25 mm. Using this, the conduction heat loads to 80 K, 20 K, and 4.5 K in a dipole magnet, due to the support posts only, are 10.52 W, 1.60 W, and 0.08 W, respectively. Table 2 lists the input parameters used in the optimization process used to determine the configuration of the current SSC support post. Table 3 lists the resulting heat loads to 80 K, 20 K, and 4.5 K for two post configurations; one utilizing G-11CR and GRP, the other utilizing only G-11CR. The current SSC support post is that represented by the first column. Note that the use of GRP reduces the 4.5 K heat load dramatically without significant impact on the 80 K and 20 K loads.

Table 2. Current SSC Support Post Input Parameters

F = 1450 kg	W = 1450 kg
F^s = 3860 kg	SF = 2.0 (safety factor)
L_1 = 376 mm	L_2 = 351 mm
L_2 = 152 mm	
E_1 = 27.6 GPa	E_2 = 68.9 GPa
ν_1 = 0.2	ν_2 = 0.2
d_1 = 179 mm	d_2 = 127 mm
σ_{u1} = 276 MPa	σ_{u2} = 413 MPa

Table 3. Comparison Of Two Optimized Post Configurations

	Outer G-11CR Inner GRP	Outer G-11CR Inner G-11CR
$Q_{300}^{4.5}$	2.77 mm	2.77 mm
	3.28 mm	5.11 mm
	2.103 W	2.038 W
	0.320 W	0.370 W
	0.015 W	0.030 W

Anchor System

The five support posts used in each SSC cryostat will share vertical and lateral loads induced by shipping and handling and seismic excitations. Thermal contraction of the cold mass assembly during warmup and cooldown necessitates axial sliding between the cold mass and each of the four outboard posts so they cannot contribute to axial load restraint. The center post is attached rigidly to the cold mass assembly to ensure correct axial position within the cryostat vacuum vessel. Given no other axial restraint, this means that the center post would see the complete axial load induced during shipping and handling, seismic disturbances, and differential pressures which can occur during magnet quenching. A single post is incapable of handling these loads alone. Utilizing a 'strong' post at the center would impose intolerable heat loads on the cryogenic systems. We require a separate means of effecting axial restraint.

One of the early anchor schemes employed in prototype SSC cryostats is shown in Fig. 4. It consists of two tubular struts connected via pinned joints at 300 K to the base of the center post and at 4.5 K to the cold mass assembly. The struts share any axial load imposed on the cold mass; one reacting in tension, the other in compression. As an anchor, this system works well. Its impact on the cryostat as a whole, however, is not ideal. First, it adds two more suspension components conducting heat from 300 K to 4.5 K, increasing the heat loads to all intercept stations. Second, it penetrates the thermal shields at 80 K and 20 K, complicating assembly and necessitating elliptical holes which are difficult to insulate. Even a small crack in the insulating layers produces an increase in radiative heat load.

Ideally one would like an anchor system with negligible thermal impact on the cryogenic systems and which introduced no perturbations into other cryostat components (like the shield holes in the case of the strut system).

Recall from a previous discussion that the sliding post/cold mass attachments implies that the fixed center post is the only one capable of resisting axial loads. Recognizing that the bending strengths of all five posts could be combined to effectively act as a single axial restraint, we have chosen to connect the 4.5 K ring of each post to that of each adjacent post with axial tie bars.

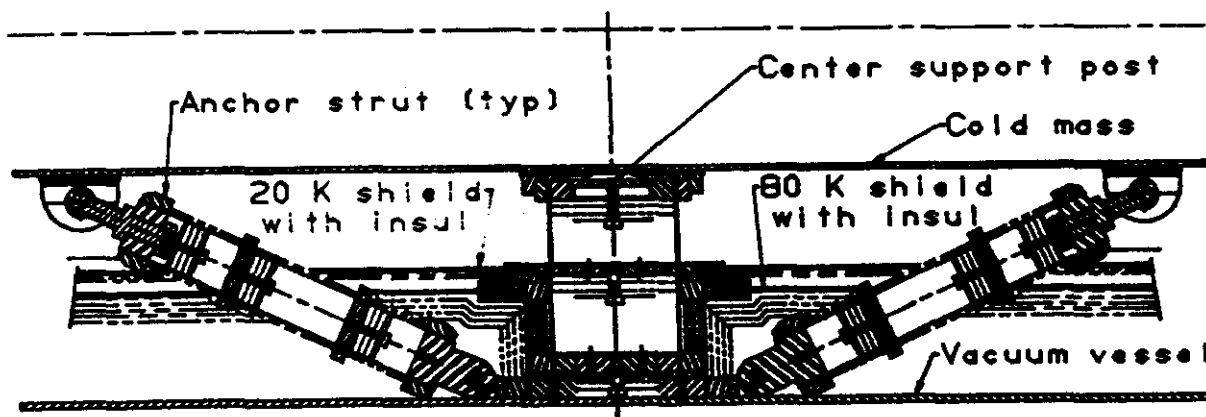


Fig. 4. Strut type axial anchor system used on SSC prototypes.

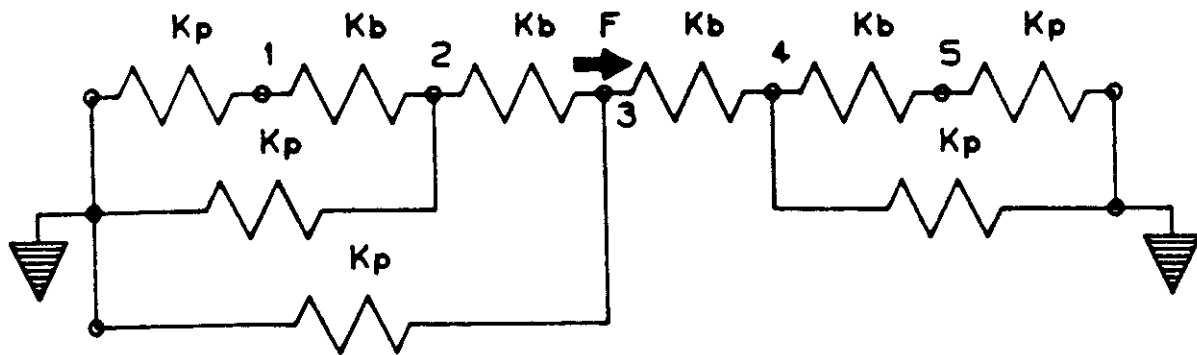


Fig. 5. Equivalent spring diagram of the post/tie bar anchor system.

To understand the effectiveness of such a scheme, we must understand the degree to which an axial load applied at the center post is shared by the remaining four posts. Specifically, we need to know the reaction forces at the top of each post, given a force applied at the center. Fig. 5 is an equivalent spring diagram of the post/tie bar system used to determine the stiffness of the total system. Points 1 through 5 represent the post/tie bar attachment points, point 3 being the top of the center post. The k_p 's represent the bending stiffness of each support posts. The k_b 's represent the axial stiffness of each tie bar. Grounded points represent the 300 K attachment of each post to the cryostat vacuum vessel.

If the tie bars were infinitely stiff one could expect the posts to share an axial load equally, i.e., for five posts, each would see one-fifth of the total. Obviously this does not represent a feasible solution. As a more realistic example, let k_p and k_b equal 1000 and 2000 kg/mm, respectively. Reaction force analysis on the system in Fig. 5 shows that 35.4% of the load goes into the center post, 19.4% goes into each of the next two outboard posts, and 12.9% goes into the two outermost posts. The total system stiffness, k_s , for this example, is 2820 kg/mm. The system efficiency may be defined as the ratio between the actual and theoretical maximum stiffnesses, $k_s/5k_p$. Using this definition, the efficiency of the system in this example is 56.4%. Increasing k_b by a factor of four yields a system whose efficiency is 69.7% so clearly one would like to make k_b as high as possible.

The remaining hurdle in the design of the post/tie bar anchor system relates to the material selection for the tie bars themselves. Materials commonly selected for use in superconducting magnet cryostats; glass composites, stainless steel, and aluminum, for example, all exhibit decreases in length when cooled from 300 K to 4.5 K. Selecting such a material for the anchor tie bars would result either in very high tensile loads in the tie bars themselves or very high bending moments in the post assemblies because of the shrinkage which occurs during cooldown. Unlike most materials, however, graphite fibers exhibit a negative coefficient of thermal expansion meaning that they grow when cooled. In most graphite composites this effect is masked by the resin system which shrinks upon cooldown, particularly if the bulk of the fibers are oriented off-axis from the measurement direction.

By pultruding graphite fibers with epoxy resin one can create a uniaxial graphite composite tube with an expansion coefficient from 300 K to 4.5 K of roughly -0.03% depending on the fiber content and on the fiber and epoxy used. Further, by attaching metallic fittings to each end of the tube which shrink upon cooldown one can produce a tube assembly with no net expansion or contraction over the prescribed temperature range. For example, a composite tube 325 cm long, with an expansion coefficient of -0.03% grow 1.0 mm when cooled from room temperature to 4.5 K. Two stainless steel ends, 16 cm long, with an expansion coefficient of 0.3%, shrink 0.5 mm each resulting in a net change in length during cooldown, for the assembly, of zero.

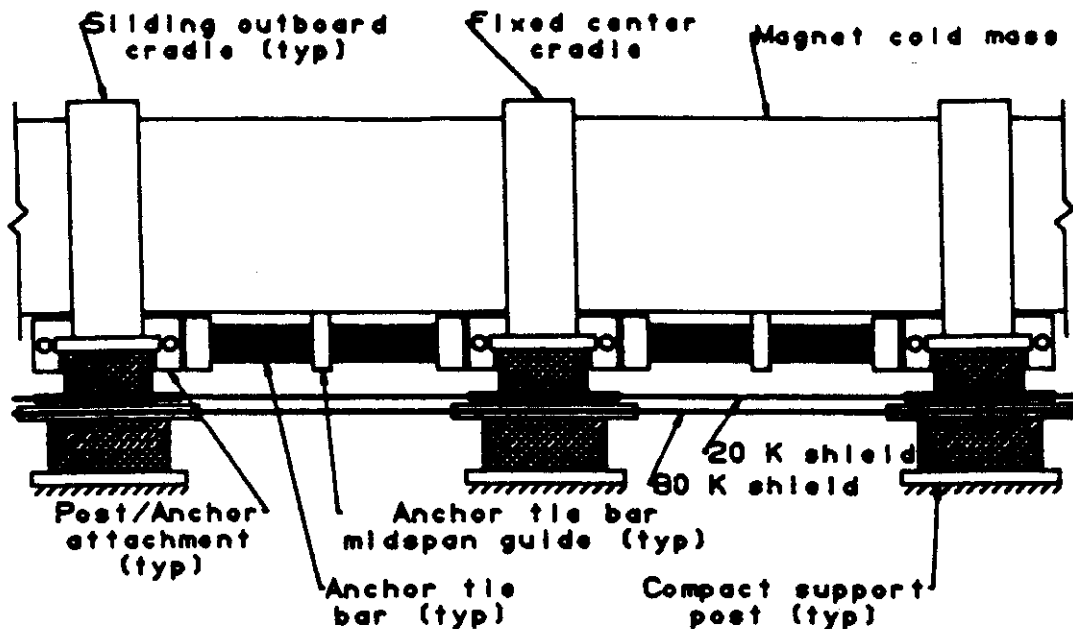


Fig. 6. Partial view of the SSC post/tie bar anchor system.

Fig. 6 illustrates the implementation of the post/tie bar anchor system employed in the current SSC dipole cryostat assembly. For clarity only the center section with two outboard posts is shown. Note that the tie bars fit completely inside the 20 K shield, eliminating the need for shield penetrations. In addition, because both ends of each tie bar assembly operate at 4.5 K, there is no added conduction heat load. Metallic fittings on each end of the tie bar assemblies are attached by the same shrink fit method used in support post fabrication.^{1,2} Also shown in Fig. 6 is a guide located midway along each tie bar. The guide is a loose fitting collar that does not restrict axial movement of the tie bar assembly, but that prevents column buckling when the tie bar is loaded in compression.

The tie bars used in the present configuration are 305 cm long tubes with an outside diameter of 64.5 mm and a wall thickness of 6.35 mm. The material is a uniaxial GRP pultrusion with an elastic modulus of 124 GPa. Using earlier notation, the calculated anchor component and system parameters are

$$\begin{aligned}
 k_p &= 1618 \text{ kg/mm} \\
 k_b &= 3690 \text{ kg/mm} \\
 k_s &= 4764 \text{ kg/mm} \\
 \text{eff} &= 58.9 \%
 \end{aligned}$$

The fixed center post sees 34.0% of the total axial load, the two outboard posts nearest the center see 19.5% each, and the outermost two posts see 13.5% each. Note that the value for F_a listed in Table 2 is 34% of the maximum quench load listed in Table 1 and represents the maximum load seen by the center support post during a magnet quench.

CONCLUDING REMARKS

The suspension system for SSC magnets has evolved toward its current configuration as the result of many design iterations, some based on established practice, others developed as complete new concepts.² The post/tie bar system is a combination of old and new. Support posts in some form have been used for many years, but none, to our knowledge, have been developed into devices which afford such low heat loads and high structural stiffnesses and strengths. Further, none have been developed using shrink fit bonds at all composite to metal joints nor have they played such an integral role in the anchor system performance. We are also unaware of the use of uniaxial graphite pultrusions in combination with metallic ends to effect axial links which are structurally sound and which exhibit little or no change in length during the temperature variations seen in superconducting magnets.

The current post/tie bar suspension system design meets the static structural requirements set forth for SSC magnets and exceeds the required thermal performance at 4.5 K. It constitutes an assembly which requires a minimum of added perturbations to other cryostat components and lends itself well to easy fabrication and mass-production. Yet to be completed is the analysis and testing related to its performance in a dynamic environment like that experienced during seismic excitations.

Our hope is that we have developed a suspension system which not only serves the needs of the SSC, but which serves to expand the current state of cryogenic suspension system design to the benefit of future applications.

ACKNOWLEDGEMENTS

The authors would like to thank Messrs. R. Zink and R. Dixon for their assistance in design development.

This work was performed at Fermi National Accelerator Laboratory which is operated by Universities Research Association Inc. under contract with the U.S. Department of Energy.

REFERENCES

1. SSC Central Design Group, "Superconducting Super Collider Magnet System Requirements," SSC-100, October 1986.
2. T.H. Nicol et al, A suspension system for superconducting super collider magnets, in: "Proceedings of the Eleventh International Cryogenic Engineering Conference," Butterworths, Surrey, UK (1986).
3. J.D. Gonczy et al, Cryogenic support thermal performance measurements, in: "Advances in Cryogenic Engineering" Vol. 33, Plenum Press, New York (to be published).
4. R.J. Roark and W.C. Young, "Formulas for Stress and Strain," Fifth Edition, McGraw Hill, New York (1975), p. 428.
5. J.R. Bensinger, Properties of cryogenic grade laminates, IEEE Conference, Boston (1979).
6. M. Takeno et al, Thermal and mechanical properties of advanced composite materials at low temperatures, in: "Advances in Cryogenic Engineering" Vol. 32, Plenum Press, New York (1986).